Electronic Structure Study of $Pr_3Ni_2O_7$ Based on Density Functional Theory

Guicong Zhao [*, #], Shenyang Chen [#], Xinyue Zhang [#]

School of Physics, Hefei University of Technology Feicui Lake Campus, Hefei, China, 230601

* Corresponding Author Email: 2778848604@qq.com

[#]These authors contributed equally.

Abstract. In the study of superconducting materials, nickelates have attracted significant attention due to their crystal structures and electronic properties resembling those of infinite-layer cuprates. The phenomenon of superconductivity was first discovered in 1911 by Dutch physicist Heike Kamerlingh Onnes, who observed that mercury exhibited zero electrical resistance near absolute zero. Subsequently, scientists proposed the BCS theory, formulated by John Bardeen, Leon Cooper, and Robert Schrieffer in 1957, which successfully explained the microscopic mechanisms of superconductivity. In 1986, George Bednorz and Alex Müller discovered the high-temperature superconductor yttrium barium copper oxide (YBCO), which has a superconducting transition temperature as high as 92 K. Recently, the synthesis and study of nickelate materials, such as $NdNiO_2$ and $Nd_{0.8}Sr_{0.2}NiO_2$, have shown superconducting transition temperatures ranging from 9 to 15 K, and high-pressure treatment has significantly increased the superconducting temperature. These advancements suggest that nickelates may possess superconducting mechanisms similar to those of cuprates, making them a hot topic of research. We chose $Pr_3Ni_2O_7$ as our research subject and employed density functional theory to calculate its band structure, finding that the d-orbitals of Ni and O play a crucial role in conductivity, with a substantial number of available electronic states for conduction.

Keywords: $Pr_3Ni_2O_7$, Electronic Properties and Structure, Superconductivity.

1. Introduction

Due to the discovery of unconventional superconductivity in infinite-layer copper oxides, an increasing number of compounds with similar crystal configurations and electronic structures have been studied in the field of superconductivity, aiming to reveal the principles of superconductivity and discover more superconductors [1,2]. A common feature of unconventional superconductors is the doping-dependent superconducting dome, which is typically close to a competing ordered phase. Given that the undoped parent compounds of nickelates and infinite-layer copper oxides share the same nominal transition metal 3d9 configuration and crystal structure [3,4], this suggests that nickelates should also be unconventional superconducting materials, making the study of nickelate superconductivity a popular trend. Subsequently, researchers have synthesized NdNiO2 and Nd0.8Sr0.2NiO2 single-crystal films by employing soft chemical topological reduction to reduce the perovskite (La327) precursor phase, achieving superconducting transition temperatures ranging from approximately 9 to 15 Kelvin, experimentally confirming the superconductivity of nickelates. To further enhance the superconducting temperature (Tc) of nickelate materials, pressure-induced Tc enhancement methods have been widely applied. For instance, $La_3Ni_2O_7$, which exhibits a Tc of 10K at ambient pressure compared to infinite-layer nickelates, achieves a Tc of 30K at 12.1GPa, and can reach approximately 80K at 14GPa [4-6]. Importantly, both single-crystal and polycrystalline samples of $La_3Ni_2O_7$ have been found to be superconducting and undergo a structural phase transition from Amam to Fmmm (or I4/mmm) at around 14-15GPa [7-9]. The fundamental electronic structure of La327 is comprised of nickel-oxygen vertex octahedra, featuring fully occupied t2g orbitals, bonding-antibonding molecular dz2 states, and nearly quarter-filled itinerant dx2−y2 states [10]. The interorbital hybridization between these two orbitals, as well as the hybridization within dz2 itself, plays a crucial role in the observed superconductivity. Based on this, this paper delves into the

electronic structure of one of the nickelates, $Pr_3Ni_2O_7$, to investigate and obtain its energy bands and state densities.

Through systematic band structure calculations, we have revealed the electronic structure characteristics of $Pr_3Ni_2O_7$, which not only deepens our understanding of the superconducting mechanism in nickelates but also helps clarify the relationship between superconductivity and electronic state distribution, providing a theoretical foundation for the study of superconductivity in other nickelates. Furthermore, the clear electronic state analysis points the way towards the discovery of new nickelate materials with higher superconducting transition temperatures, potentially stimulating research on other similar compounds and advancing the development of novel superconductors. Additionally, our research demonstrates the effectiveness of density functional theory (DFT) in studying the electronic structures of complex materials, particularly in exploring the electronic properties of unconventional superconductors, providing methodological references for future related studies. This work offers new perspectives for researchers in materials science, condensed matter physics, and computational materials science, fostering collaboration and communication across disciplines. It also contributes new experimental and theoretical data to the fundamental scientific research of nickelate materials, aiding in the further understanding of their properties and potential applications.

2. Density functional theory

Density Functional Theory (DFT) is a quantum mechanical computational method based on the Hohenberg-Kohn theorem, which states that the ground state electron density of a system uniquely determines the external potential and all physical properties of the system. The core of DFT lies in transforming complex multi-electron problems into single-electron problems. By solving the Kohn-Sham equations, DFT approximates the electronic structure, allowing for the calculation of the system's ground state energy and density.

2.1. Hartree-Fock approximation

Using the adiabatic approximation, the multi-electron Schrödinger equation:

$$\{\sum_i \left[-\frac{\hbar^2}{2m}\nabla_i^2 - \frac{1}{4\pi\varepsilon_0}\sum_i \frac{e^2}{|r-R_i|}\right] + \frac{1}{8\pi\varepsilon_0}\sum_{i,j}\frac{e^2}{|r_i-r_j|}\}\psi = \left[\sum_i \hat{H}_i + \sum_{i,j}\hat{H}_{ij}\right]\psi = E\psi \quad (1)$$

For ease of solving, the Hamiltonian operator is decomposed into single-particle $\hat{H}_i$ and two-particle $\hat{H}_{ij}$ operators. Ignoring the two-particle operator allows the multi-electron Schrödinger equation to be simplified to:

$$\sum \hat{H}_i \psi = E\psi \quad (2)$$

2.2. The Hohenberg-Kohn theorem

The Hamiltonian for an N-electron system is given by:

$$\hat{\mathbf{H}} = \hat{\mathbf{T}} + \hat{\mathbf{U}} + \hat{\mathbf{V}} \quad (3)$$

Where $\hat{\mathbf{T}}$ is the kinetic energy term, $\mathbf{U}$ represents the Coulomb interactions, and $\mathbf{V_{ea}}$ is the external potential acting on the electrons, which in solids can be equivalent to the effect of the ionic lattice on the electrons.

$$\mathbf{V_{ext}} = \sum_i \mathbf{v_{ext}}(\mathbf{r_i}) \quad (4)$$

$$\mathbf{v_{ext}} = -\frac{1}{4\pi\varepsilon_0}\sum_l \frac{\mathbf{Z_l e^2}}{|\mathbf{r}-\mathbf{R_l}|} \quad (5)$$

Here, $\mathbf{Z_l}$ is the amount of positive charge associated with the ionic lattice at position $\mathbf{R_l}$. The corresponding Schrödinger equation is:

$$\widehat{\mathbf{H}}|\boldsymbol{\psi}(\mathbf{r_1}, \mathbf{r_2}, \ldots, \mathbf{r_N})\rangle = \boldsymbol{\varepsilon}|\boldsymbol{\psi}(\mathbf{r_1}, \mathbf{r_2}, \ldots, \mathbf{r_N})\rangle \tag{6}$$

The electron density is defined as:

$$\boldsymbol{\rho}(\mathbf{r}) = \langle \boldsymbol{\psi}(\mathbf{r_1}, \mathbf{r_2}, \ldots, \mathbf{r_N})| \sum_{\mathbf{i}} \boldsymbol{\delta}(\mathbf{r} - \mathbf{r_i})|\boldsymbol{\psi}(\mathbf{r_1}, \mathbf{r_2}, \ldots, \mathbf{r_N})\rangle \tag{7}$$

We can rewrite the external potential as a $\boldsymbol{\delta}$ function:

$$\mathbf{V_{ext}} = \sum_{\mathbf{i}} \int \mathbf{v_{ext}}(\mathbf{r})\boldsymbol{\delta}(\mathbf{r} - \mathbf{ri})\mathbf{dr} \tag{8}$$

By combining the above equations,

$$\langle \boldsymbol{\psi}|\mathbf{V_{ext}}|\boldsymbol{\psi}\rangle = \int \boldsymbol{\nu}_{\mathbf{ext}}(\mathbf{r})\boldsymbol{\rho}(\mathbf{r})\mathbf{dr} \tag{9}$$

We can derive that if the external potential v_{ca} or the electron density $V_{ca}(r)$ is known, in principle, we can obtain the ground state wave function $|\psi\rangle$ by solving the Schrödinger equation, allowing us to calculate $\rho(r)$. This density $\rho(r)$ can be viewed as a functional of $v_{ext}(r)$, which means:

$$\boldsymbol{\rho}(\mathbf{r}) = \mathbf{F}[\boldsymbol{\nu}_{\mathbf{ext}}(\mathbf{r})] \tag{10}$$

2.3. Kohn-Sham equation

Replace the kinetic energy functional $T[\rho]$with $T_s[\rho]$that of a non-interacting particle, ensuring both have the same density distribution function. Additionally, assign the non-convertible part of the difference between T and Ts to an unknown term of $E_{xc}[\rho]$. This allows us to obtain a single-particle wave function. According to the variational principle, we can derive the corresponding Schrödinger equation:

$$\left[-\frac{\hbar^2}{2\mathbf{m}}\boldsymbol{\nabla}^2 + \mathbf{V}(\mathbf{r})\right]\boldsymbol{\varphi}_{\mathbf{i}}(\mathbf{r}) = \boldsymbol{\varepsilon}_{\mathbf{i}}\boldsymbol{\varphi}_{\mathbf{i}}(\mathbf{r}) \tag{11}$$

Of which:

$$\begin{aligned}\mathbf{V_{KS}}(\mathbf{r}) &= \frac{\mathbf{1}}{\mathbf{4\pi\varepsilon_0}}\int \frac{\mathbf{e^2}}{|\mathbf{r}-\mathbf{r}'|}\boldsymbol{\rho}(\mathbf{r}')\mathbf{dr}' + \boldsymbol{\nu}_{\mathbf{ext}}(\mathbf{r}) + \boldsymbol{\nu}_{\mathbf{xc}}(\mathbf{r}) \\ &= \boldsymbol{\nu}_{\mathbf{Coul}}(\mathbf{r}) + \boldsymbol{\nu}_{\mathbf{ext}}(\mathbf{r}) + \boldsymbol{\nu}_{\mathbf{xc}}(\mathbf{r})\end{aligned} \tag{12}$$

Exchange correlation expression:

$$\boldsymbol{\nu}_{\mathbf{xc}}(\mathbf{r}) \equiv \frac{\boldsymbol{\delta}\mathbf{E_{xc}}[\boldsymbol{\rho}(\mathbf{r})]}{\boldsymbol{\delta}\boldsymbol{\rho}(\mathbf{r})} \tag{13}$$

2.4. Exchange-correlation functional

The Local Density Approximation (LDA) is an effective method used in density functional theory to calculate exchange-correlation energy. It is based on the uniform electron gas model, approximating the exchange-correlation energy functional of a non-uniform electron gas by the value from a uniform system. Although finding an accurate exchange-correlation energy functional is challenging, LDA has proven to be very successful in many specific calculations due to its simple expression and practicality. As a result, LDA plays an important role in addressing the ground state properties of many-electron systems and has become a crucial component of density functional theory. Under the LDA approximation, $E_{xc}[\rho]$ can be written as:

$$\mathbf{E_{XC}^{LDA}}[\boldsymbol{\rho}] = \int \mathbf{dr}\boldsymbol{\rho}(\mathbf{r})\boldsymbol{\varepsilon}_{\mathbf{XC}}[\boldsymbol{\rho}(\mathbf{r})] \tag{14}$$

The exchange-correlation potential is expressed in terms of the exchange-correlation energy density$\boldsymbol{\varepsilon}_{\mathbf{xc}}$:

$$\boldsymbol{\nu}_{\boldsymbol{\chi}\mathbf{C}}(\mathbf{r}, \boldsymbol{\rho}) = \frac{\boldsymbol{\delta}\mathbf{E}_{\boldsymbol{\chi}\mathbf{C}}[\boldsymbol{\rho}(\mathbf{r})]}{\boldsymbol{\delta}\boldsymbol{\rho}(\mathbf{r})} = \boldsymbol{\varepsilon}_{\boldsymbol{\chi}\mathbf{C}}(\mathbf{r}, \boldsymbol{\rho}) + \int \mathbf{dr}\boldsymbol{\rho}(\mathbf{r}')\frac{\boldsymbol{\delta}\boldsymbol{\varepsilon}_{\boldsymbol{\chi}\mathbf{C}}(\mathbf{r}', \boldsymbol{\rho})}{\boldsymbol{\delta}\boldsymbol{\rho}} \tag{15}$$

Obtained using the Local Density Approximation:

$$\boldsymbol{\nu_{xc}(r,\rho) = \varepsilon_{xc}(\rho) + \rho\frac{d\varepsilon_{xc}(\rho)}{d\rho}} \tag{16}$$

$$\boldsymbol{\rho = \frac{3}{4\pi r_s^3}} \tag{17}$$

Expressed as a function of $\mathbf{r_s}$:

$$\boldsymbol{\nu_{\chi C}(r_s) = \varepsilon_{\chi C}(r_s) - \frac{r_s}{3}\frac{d\varepsilon_{\chi C}(r_s)}{dr_s}} \tag{18}$$

Ignoring the correlation effects in the uniform electron gas results in a relatively simple form for the exchange-correlation energy density of electrons in a uniform electron gas at the same density

$$\boldsymbol{\varepsilon_C = \frac{3e^2}{4\pi\alpha r_s}} \tag{19}$$

Obtain the exchange-correlation potential of the non-uniform electron gas:

$$\boldsymbol{\nu_X(r_s) = \frac{4}{3}\varepsilon_X(r_s)} \tag{20}$$

Clearly, the local density approximation is strictly valid only in the state of a uniform electron gas.

2.5. Solving the Kohn-Sham equations

According to DFT theory, the key to solving the problem lies in how to solve the Kohn-Sham equations. Typically, a self-consistent iterative method is employed. First, an appropriate initial electron density function$\rho_{in}(r)$ is chosen, which can be generated randomly. Then, based on this density function, the effective potential $V_{ks}(r)$ in the Kohn-Sham equations is calculated, allowing for the determination of related values $\nu_{ext}(r), \nu_{Coul}(r), \nu_{xc}(r)$ and the single-particle eigenfunctionsφ_i.Next, the new charge density function$\rho_{out}(r)$ is computed using the eigenfunctions. After that, the new and old charge density functions are compared. If the new charge density function has converged, the total energy is calculated, and the results are output. If it has not converged, the previous two charge density functions are averaged with weights to generate a new trial density function, and the next iteration begins, continuing until convergence is achieved.

3. Energy band analysis

To better analyze the electronic structure of $Pr_3Ni_2O_7$ in figure 1, we conducted density functional theory (DFT) calculations. The band diagram reflects the occupation of electronic orbitals, with the bands below the Fermi level representing the occupied orbitals. In $Pr_3Ni_2O_7$, all 3d orbitals of $Ni^{+2.5}$ are occupied, but d_{xz}, d_{yz} and d_{xy} orbitals exhibit relatively lower energies, while the $d_{x^2-y^2}$ and d_{Z^2} orbitals have higher energies. This energy splitting is attributed to the presence of the lattice structure, which splits the $Ni^{+2.5}$ energy levels into two groups: e_g and t_{2g}, higher-energy orbitals(e_g)including $d_{x^2-y^2}$and d_{Z^2}, and lower-energy orbitals(t_{2g})including d_{xz}, d_{yz}, andd_{xy}, which are fully occupied by electrons. Additionally, the Jahn-Teller effect causes the stretching of Ni's Z-orbitals, resulting in higher energies for the and orbitals compared to the orbitals. Within the bilayer structure, a bandgap exists, and the overlap between the Z-orbitals of Ni and O splits the Ni orbitals into bonding-antibonding molecular d_{Z^2}states. The bonding state, having a lower energy, is fully occupied and forms relatively flat ionic bands along the Γ-X and Γ-Y directions, which is a characteristic feature of electronic σ-bonds. In contrast, $d_{x^2-y^2}$ band remains degenerate and is quarter-filled. Based on the general assumption of the crucial role of the electronic properties in the emergence of superconductivity in $Pr_3Ni_2O_7$, we hypothesize that applying high pressure (14GPa) could lead to the metallization of the σ-bond bands below the Fermi level through hole doping on

d_{Z^2} orbitals and electron doping on$d_{x^2-y^2}$orbitals. This metallization would potentially enable the observation of superconductivity in $Pr_3Ni_2O_7$.

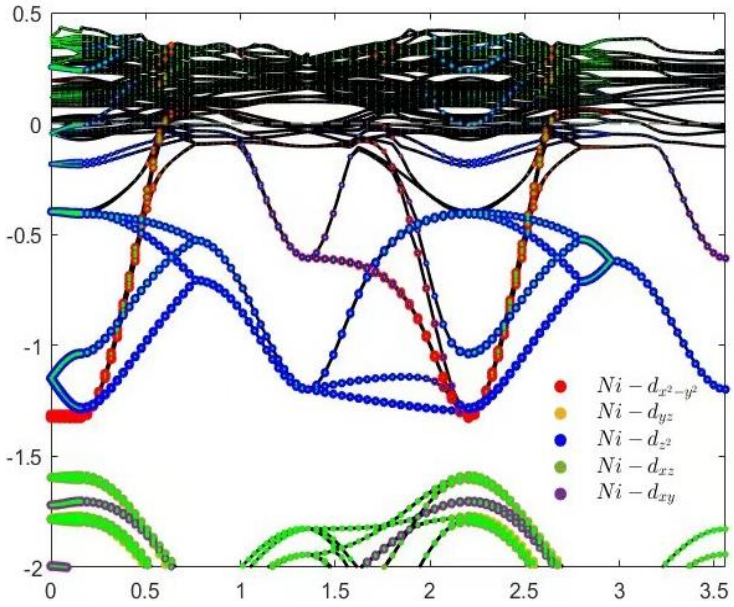

Figure 1. Energy Band Diagram

4. Density of states analysis

The state density refers to the number of electronic states within a unit energy range. In the band structure of solids, different energies correspond to different electronic state densities, and a higher state density generally indicates better conductivity. In Figure 2, we have utilized density functional theory to obtain the state densities of different elements in $Pr_3Ni_2O_7$ at various energies. The total state density and the state density of Pr exhibit a high degree of overlap at the Fermi energy level. Figure 3 further reveals that the state density below the Fermi level is greater than that above it, indicating that more electrons occupy lower energy states. Consequently, there are relatively more holes available in the valence band to participate in electrical conduction, enhancing the conductivity of $Pr_3Ni_2O_7$ to a certain extent. Moreover, the presence of several peaks and troughs in the state density below the Fermi level suggests that the distribution of electrons among different energy states is diverse and complex, reflecting the complex structure of $Pr_3Ni_2O_7$.

At the Fermi level, the state density exhibits a significant distribution with a pronounced peak, indicating active electrons and strong electronic correlations. This suggests that $Pr_3Ni_2O_7$ possesses a certain level of conductivity in this state. Among the elements, Ni and O have the highest state densities at the Fermi level, implying that the conductivity of $Pr_3Ni_2O_7$ is primarily determined by Ni and O. For Ni, the orbitals with higher state densities are $d_{x^2-y^2}$, d_{Z^2} and d_{xy},indicating that these orbitals play a dominant role in the conductivity of $Pr_3Ni_2O_7$, consistent with previous molecular orbital theory analyses.

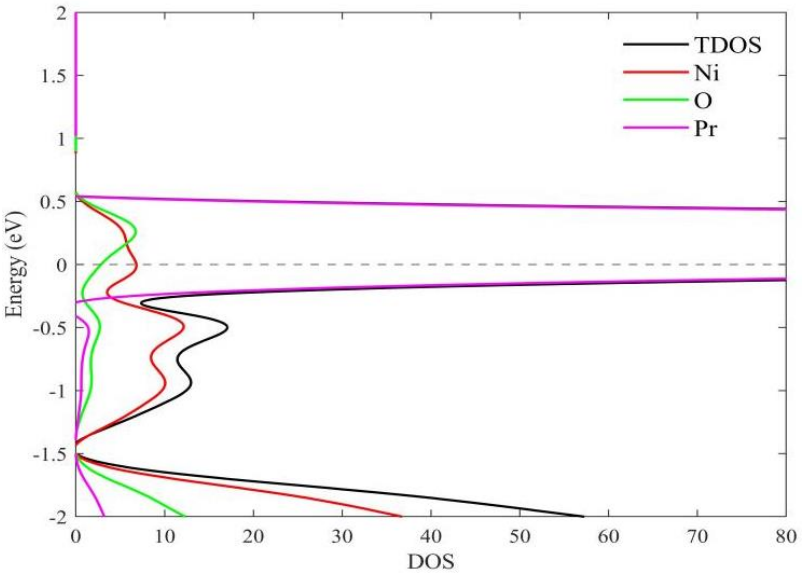

Figure 2. Total Elemental State Density

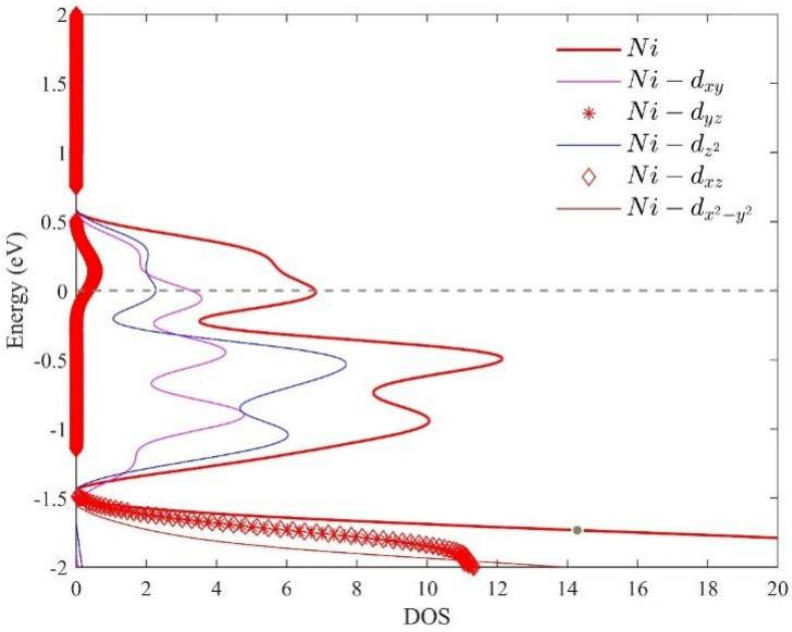

Figure 3. State Density of Ni Element

5. Conclusion

Through density functional theory calculations, we obtained the band structure and density of states (DOS) distribution of $Pr_3Ni_2O_7$ under high-pressure conditions. These studies reveal its internal electronic distribution and structural characteristics. The band structure shows that all 3d orbitals are fully occupied, with the $d_{x^2-y^2}$, d_{Z^2} and d_{xy} orbitals having relatively low energy, while the $d_{x^2-y^2}$ and d_{Z^2} orbitals have higher energy. This characteristic indicates that the material exhibits significant electronic σ-bonding properties, with bonding electronic states forming relatively flat ionic bands along the Γ-X and Γ-Y directions. Analysis of the DOS distribution reveals a high density of states near the Fermi level for both Ni and O, indicating that the conductivity of $Pr_3Ni_2O_7$ is primarily influenced by these two elements. In particular, for the Ni element, the orbitals with high density of states include d_{xy}, d_{yz}, and d_{xz}, further indicating that these three orbitals play a dominant role in the conductivity of $Pr_3Ni_2O_7$. These results are consistent with previous molecular orbital

theory analyses, reinforcing the critical contribution of Ni and its specific orbitals to the electronic and transport properties of the material. Based on these findings, we believe that $Pr_3Ni_2O_7$ has high feasibility for applications in electronic devices and superconducting materials. Its unique electronic properties and good conductivity make it a potential material for quantum computing, efficient energy transmission, and other cutting-edge technological fields. In practical applications, optimizing the synthesis methods of $Pr_3Ni_2O_7$ and adjusting external pressure conditions are expected to further enhance its conductivity, thereby improving its reliability and efficiency in electronic devices.

References

[1] D. Li, K. Lee, B. Y. Wang, et al. Superconductivity in an infinite-layer nickelate [J]. Nature, 2019, 572 (7771): 624 - 627.

[2] Liu, Z. et al. Evidence for charge and spin density waves in single crystals of La3Ni2O7 and La3Ni2O6. Sci. Chin. Phys. Mech. Astron. 2023, 66 (5): 217411.

[3] Huo, M. et al. Synthesis and properties of La1–xSrxNiO3 and La1–xSrxNiO2. Chin. Phys. B 2022, 31 (10): 107401.

[4] D. Li, B. Y. Wang, K. Lee, et al. Superconducting dome in Nd1- xSrxNiO2 infinite layer films [J]. Physical Review Letters, 2020, 125 (2): 027001.

[5] H. Sun, M. Huo, X. Hu, et al. Signatures of superconductivity near 80 K in a nickelate under high pressure [J]. Nature, 2023, 621 (7979): 493 - 498.

[6] Y. Zhang, D. Su, Y. Huang, et al. High-temperature superconductivity with zero resistance and strange metal behavior in La3Ni2O7 [J]. Nature Physics, 2024, 20: 1269 – 1273.

[7] J. Hou, P. T. Yang, Z. Y. Liu, et al. Emergence of high-temperature superconducting phase in the pressurized La3Ni2O7 crystals [J]. Chinese Physics Letters, 2023, 40 (10): 117302.

[8] G. Wang, N. N. Wang, J. Hou, et al. Pressure-induced superconductivity in the La3Ni2O7 -polycrystalline samples [J]. Physical Review X, 2024, 14 (1): 011040.

[9] N. N. Wang, M. W. Yang, Z. Yang, et al. Pressure-induced monotonic enhance-ment of Tc to over 30 K in superconducting Pr0.82Sr0.18NiO2 thin films [J]. Nature Communications, 2022, 13: 4367.

[10] C. Lu, Z. Pan, F. Yang, et al. Interlayer coupling driven high-temperature superconductivity in La3Ni2O7 under pressure [J]. Physical Review Letters, 2024, 132 (14): 146002.